

## ORIGINAL RESEARCH ARTICLE

# Synthesis and application of nano-MH/MPB as intumescent flame retardant (IFR)

Aiming Zhao, Yanmao Dong, Qiuyang Ni, Zhiyu Bao\*

School of chemistry and Bioengineering, Suzhou University of Science and Technology, Suzhou 215009, Jiangsu, China.  
E-mail: bzy1952@126.com

### ABSTRACT

Magnesium hydroxide/melamine phosphate borate (nano MH/MPB), a novel nano-composition intumescent flame retardant, was synthesized with the in-situ reaction method from  $\text{MgCl}_2 \cdot 6\text{H}_2\text{O}$  sodium hydroxide (NaOH) and melamine phosphate borate (MPB) in the absence of  $\text{H}_2\text{O}$ . The structure of the product was confirmed by EDAX IR and XRD. The effects of reaction temperature and time on the dimension of magnesium hydroxide were observed. The effects of mass ratio of magnesium hydroxide to MPB on the flame retardancy of nano-MH/MPB/EP were examined with the limiting oxygen test. The results show that the optimal condition of synthesis of MH/MPB is  $\text{mMH/mMPB} = 0.25$ , reacting under  $75^\circ\text{C}$  for 30 minutes. Finally, the mechanism for flame retardancy of nano-MH/MPB/EP was pilot studied by means of IR of char layer and TG of MH/MPB.

**Keywords:** Intumescent Flame Retardant; Magnesium Hydroxide; Nano-Composition; Melamine Phosphate Borate; Synergistic Agents

### ARTICLE INFO

Received: 23 April 2021  
Accepted: 16 June 2021  
Available online: 23 June 2021

### COPYRIGHT

Copyright © 2021 Aiming Zhao, *et al.*  
EnPress Publisher LLC. This work is licensed under the Creative Commons Attribution-NonCommercial 4.0 International License (CC BY-NC 4.0).  
<https://creativecommons.org/licenses/by-nc/4.0/>

## 1. Introduction

In recent years, intumescent flame-retarded (IFR) has become a research hotspot because of its high thermal stability and environmental friendliness<sup>[1]</sup>. IFR is mainly composed of carbon source (such as pentaerythritol), acid source (such as ammonium polyphosphate) and gas source (such as melamine), which can be divided into mixed type and simple type. Among them, hybrid IFR has some disadvantages, such as easy moisture absorption, poor thermal stability, low flame-retarded efficiency and difficult compatibility with polymers<sup>[2]</sup>. Simple IFR can effectively solve the above problems, but it also has the disadvantages of single element composition and high cost.

In order to improve the above problems, IFR and nanoparticles can be used as flame-retarded polymers. Nanoparticles have the characteristics of high surface atomic ratio, large specific surface area and good dispersion, showing a unique volume effect and surface effect<sup>[3]</sup>, which can improve the mechanical properties and flame-retarded properties of materials. It is reported that clay<sup>[4,5]</sup>, nano magnesium hydroxide (MH)<sup>[6]</sup>, nano aluminum hydroxide<sup>[7]</sup>, nano  $\text{SiO}_2$ <sup>[8]</sup>, nano zinc oxide (ZnO)<sup>[9,10]</sup>, nano  $\text{TiO}_2$  can be used as synergistic agents of IFR to flame-retarded PP, PE, PA66, etc.<sup>[11]</sup> However, the current research mainly focuses on Intumescent clay nanocomposite flame-retarded PP and PA66<sup>[12]</sup>.

Magnesium hydroxide (MH) decomposes at 340–490 °C, and the initial decomposition temperature is 100 °C higher than that of Al(OH)<sub>3</sub>; the heat absorption capacity of 1.37kJ·g<sup>-1</sup> is higher than that of Al(OH)<sub>3</sub> (1.17kJ·g<sup>-1</sup>), and the heat capacity is also 17%, which is helpful to improve the flame-retarded efficiency<sup>[13,14]</sup>; in addition, magnesium hydroxide is a good smoke suppressant<sup>[15]</sup>. Nano MH was introduced into IFR system to flame-retarded EP for the first time to improve the disadvantages of IFR, such as low flame-retarded efficiency and incompatibility with materials. Nano MH/MPB intumescent nanocomposite flame-retarded was prepared by in-situ generation method. The flame-retarded synergistic effect of MH and MPB in EP was studied.

## 2. Experiment

### 2.1 Main raw materials

Melamine phosphate borate (MPB), self-made (as shown in **Figure 1**)<sup>[16]</sup>; MgCl<sub>2</sub>·6H<sub>2</sub>O, analytical reagent, produced by Shanghai Tongya Chemical Technology Development Co., Ltd; ethylenediamine, analytical pure, produced by Shanghai Qiangshun Chemical Co., Ltd; E-44 epoxy resin (EP), produced by Zhenjiang Danbao Resin Co., Ltd.

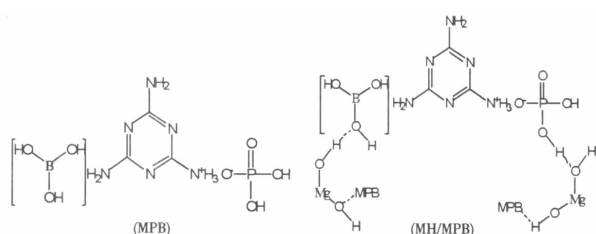


**Figure 1.** Sketch pattern of MPB and MH/MPB.

### 2.2 Synthesis of MH/MPB

MPB, MgCl<sub>2</sub>·6H<sub>2</sub>O and water are added into a three-mouth bottle in a certain proportion, heated and stirred, and completely dissolved by ultrasonic oscillation. Then, slowly drop the prepared precipitant NaOH solution into the aqueous solution of MPB and MgCl<sub>2</sub>·6H<sub>2</sub>O, gradually appear white turbidity, ultrasonic oscillation, stirring and holding for a period of time. Cool, filter, wash with water and absolute ethanol until there is no CL (AgNO<sub>3</sub> detection), dry

at 60 °C and weigh.

### 2.3 Preparation of flame-retarded epoxy resin samples of MH/MPB

Ethylenediamine was used as curing agent, 10 g epoxy resin and 1 g ethylenediamine were mixed at room temperature, stirred evenly, and a certain amount of MH/MPB flame-retarded was added. After stirring evenly, it is injected into a self-made aluminum mold with specific size, cured at room temperature for 24 hours, and then cured at 80 °C for 2 hours. After complete curing, it shall be trimmed into the required spline for testing.

### 2.4 Testing and characterization

1) The products were detected by Prostar LC240 infrared spectrometer (KBr tablet pressing method).

2) The X-ray powder diffraction test is continuously scanned on the German Bruker D8 X-ray diffractometer for XRD test. The test conditions are: Cu target, rear monochrome tube, 45 kV of tube pressure, 20 mA of tube flow, scanning ranging 10° ≤ 2θ ≤ 80°, 4°·min<sup>-1</sup> of scanning speed.

3) The elemental composition of the product was detected by S-570 scanning electron microscope (SEM) (equipped with edaxpv9900 energy spectrometer).

4) The oxygen index test (LOI) adopts HC900-2 oxygen index tester according to GB/T 2406-93, and the flame-retarded epoxy resin spline size is 110 mm × 6 mm × 3.5 mm; limiting oxygen index test is conducted.

5) American Pekin Elmer TGA7 thermogravimetric analyzer is used for thermogravimetric analysis.

## 3. Results and discussion

### 3.1 Theory

MPB molecules contain -NH<sub>2</sub>, -OH, P=O and other groups. These groups can form hydrogen bonds with -OH of nano MH (as shown in **Figure 1**). At the same time, nanoparticles have high activity and are easy to combine with macromolecules. In this way, nano MH/MPB intumescent nanocomposite

flame-retarded was prepared by combining MH and MPB through chemical and physical effects.

### 3.2 Infrared spectrum analysis

The infrared spectra of MH, MPB and MH/MPB are shown in **Figure 2**. Infrared spectrum analysis is as follows<sup>[17]</sup>: in **Figure 2a**,  $3,698\text{ cm}^{-1}$  is O-H stretching absorption peak in the MH crystal structure,  $1,467\text{ cm}^{-1}$  is the bending vibration absorption peak of -OH, and the wide absorption peak near  $1,643\text{ cm}^{-1}$  and  $3,413\text{ cm}^{-1}$  should be the absorption peak of  $\text{H}_2\text{O}$  in MH crystal. This result is consistent with the MH results reported in literature<sup>[18]</sup>. **Figure 2c** is obviously different from **Figures 2a** and **2b**. In **Figure 2c**, there are not only the O-H stretching absorption peak  $3,702\text{ cm}^{-1}$  in MH structure, but also the overlapping  $3,339\text{ cm}^{-1}$  and  $3,132\text{ cm}^{-1}$  of N-H stretching vibration absorption peaks in  $-\text{NH}_3^+$ , -OH and  $-\text{NH}_2$  in MPB structure, P=O stretching vibration absorption peak  $1,265\text{ cm}^{-1}$ , C=N stretching vibration absorption peak  $1,656\text{ cm}^{-1}$ . This shows that MH/MPB composite flame-retarded was prepared.

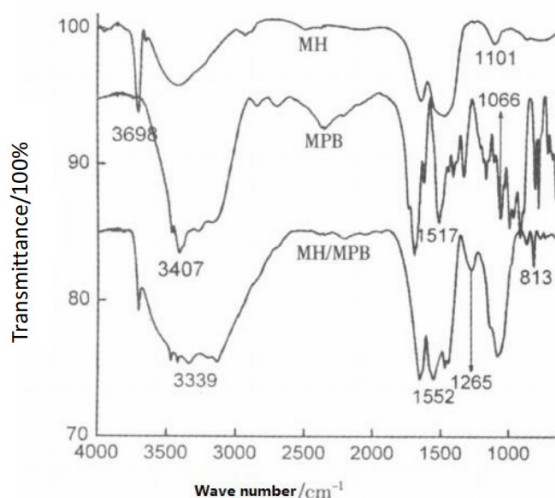


**Figure 2.** Infrared spectrum of MH/MPB and MH/MPB.

### 3.3 Elemental analysis

The energy spectrum of MHMPB (mMH/mMPB = 0.25) is shown in **Figure 3**. It can be seen from **Figure 3** that the product mainly contains C, N, O, P, Mg and other elements, which further confirms the preparation of MH/MPB composite flame-retarded.

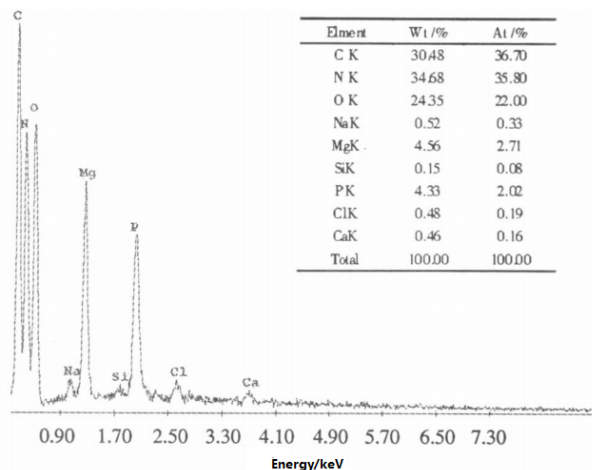


**Figure 3.** Energy spectrum of MH/MPB (mMH/mMPB).

### 3.4 XRD analysis of MH, MPB and MH/MPB

The XRD spectra of MH, MPB and MH/MPB are shown in **Figure 4**. It can be seen from the comparison of the diffraction peak positions of **Figure 4C** with **Figure 4A** and **Figure 4B** that in **Figure 4C**, MPB and  $\text{Mg}(\text{OH})_2$  diffraction peaks exist. Thus, the preparation of MH/MPB complex was further confirmed. The diffraction peak position of crystal plane of MH's (001), (100), (101) in **Figure 4C** is obvious and widened, indicating that the particle size is small<sup>[19]</sup>. The grain size can be determined by XRD using Scherrer formula. The peak is calculated to obtain, and the calculation results are shown in **Table 1**<sup>[20]</sup>. The calculated results show that  $\text{Mg}(\text{OH})_2$  in the prepared MH/MPB composite has reached nano level.

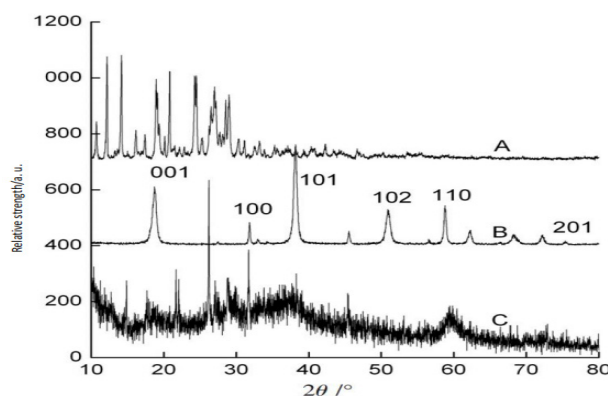


**Figure 4.** XRD spectra of MH, MPB and MH/MPB (A: MPB; B: MH; C: MH/MPB).

**Table 1.** Grain size of MH/MPB

2 $\theta$ / $^{\circ}$	Crystal plane/hkl	Half peak width/ $^{\circ}$	Grain size/nm
17.72	001	0.33	24.12
31.70	100	0.19	43.03
38.24	101	0.15	55.51
59.34	110	0.40	20.12

### 3.5 Effect of reaction temperature on grain size of MH/MPB

Using single factor experimental analysis, keep other influencing factors unchanged, change the reaction temperature to 35  $^{\circ}\text{C}$ , 45  $^{\circ}\text{C}$ , 55  $^{\circ}\text{C}$ , 65  $^{\circ}\text{C}$  and 75  $^{\circ}\text{C}$ , and compare the effect of MH/MPB XRD spectrum (**Figure 5**), and the grain size is calculated and compared by Scherrer formula (**Table 2**).

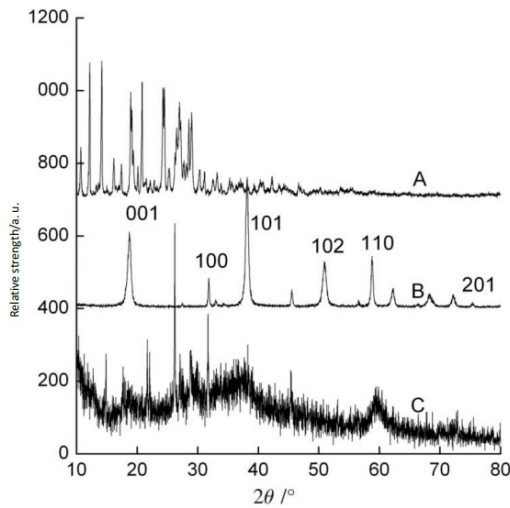


**Figure 5.** XRD patterns of MH/MPB at different reaction temperatures (A: 35  $^{\circ}\text{C}$ ; B: 45  $^{\circ}\text{C}$ ; C: 55  $^{\circ}\text{C}$ ; D: 65  $^{\circ}\text{C}$ ; E: 75  $^{\circ}\text{C}$ ).

**Figure 5** shows that when the temperature is too high, the diffraction peak is obviously refined,

indicating that the grain size becomes larger, and the change of (201) crystal plane is obvious. In addition, it can be concluded from **Table 2** that when the stress temperature is lower than 75  $^{\circ}\text{C}$ , the grain size of MH/MPB decreases slightly with the increase of temperature; when the reaction temperature reaches 75  $^{\circ}\text{C}$ , the grain size of MH/MPB increases sharply. This is because the reaction temperature has an effect on the formation and growth of nuclei<sup>[21]</sup>. The nucleation rate in low temperature region is higher than that in crystal. The growth rate is fast, that is, low temperature is conducive to the formation of crystal nucleus, which is not conducive to the growth of crystal nucleus. Generally, fine crystals are obtained; as the temperature increases, the solubility decreases. The viscosity of the liquid increases the mass transfer coefficient and greatly improves the crystal growth rate, so as to increase the crystal nucleus. When the temperature exceeds 75  $^{\circ}\text{C}$ , the crystal nuclei agglomerate and the grain size increases sharply.

### 3.6 Effect of reaction time on grain size of MH/MPB

Keep other influencing factors unchanged, change the reaction time to 10, 20, 30, 40 and 50 minutes, and compare the XRD spectra of MH/MPB (**Figure 6**). The grain size is calculated and compared by Scherrer formula (**Table 3**). As shown in **Figure 6**, when the reaction time is less than 30 min, the diffraction peak broadening is obvious, indicating that the grain size is small; more than 30 minutes, the diffraction peak is obviously refined, indicating

**Table 2.** Grain size of MH/MPB at different reaction temperatures

Temperature / $^{\circ}\text{C}$	Crystal plane / hkl	2 $\theta$ / $^{\circ}$	Half peak width / $^{\circ}$	Grain size / nm	Average size /nm	Temperature / $^{\circ}\text{C}$	Crystal plane / hkl	2 $\theta$ / $^{\circ}$	Half peak width / $^{\circ}$	Grain size /nm	Average size /nm
35	001	17.86	0.40	19.91	26.50	65	001	17.76	0.50	15.92	21.93
	100	31.76	0.25	32.71			100	31.74	0.37	22.10	
	101	38.48	0.31	26.88			101	38.34	0.30	22.76	
45	001	17.86	0.26	30.61	27.53	75	001	17.94	0.13	61.23	51.39
	100	31.72	0.41	19.94			100	31.74	0.20	40.89	
	101	38.46	0.26	32.04			101	38.32	0.16	52.05	
55	001	18	0.28	28.44	23.80						
	100	31.84	0.40	20.45							
	101	38.46	0.37	22.52							

that the grain size becomes larger; (101) and (110) crystal planes change significantly. This moment the image is confirmed by **Table 3**. When the reaction time is 30 minutes, the grain size of MH/MPB is the smallest, close to 19 nm. The reaction speed between magnesium chloride and sodium hydroxide is very fast, and the whole reaction can be completed in an instant. At the initial stage of the reaction, fine MH is easy to agglomerate and form larger MH; but with the extension of time, the energy and activity of MH crystal increase, and the smaller MH can be removed from the larger MH crystal separated to form MH particles with small particle size<sup>[22]</sup>. If the reaction time is too long, MH particles will agglomerate again. So it's not easy to react too short or too long and the optimum reaction time is 30 minutes.

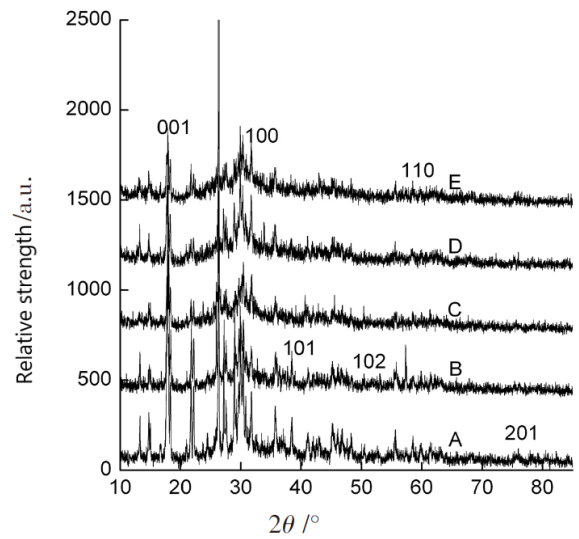


**Figure 6.** XRD pattern of MH / MPB at different reaction times.

**Table 3.** Grain size of MH/MPB at different reaction temperatures

Temperature /°C	Crystal plane / hkl	2θ/°	Half peak width /°	Grain size /nm	Average size /nm	Temperature /°C	Crystal plane / hkl	2θ/°	Half peak width /°	Grain size /nm	Average size /nm
10	001	17.74	0.14	58.86	37.86	40	001	17.82	0.16	49.76	48.94
	101	37.66	0.24	34.63			101	37.92	0.14	59.41	
	110	59.32	0.45	20.11			110	58.96	0.24	37.65	
20	001	17.72	0.33	24.12	34.08	50	001	17.7	0.13	61.24	90.48
	101	38.24	0.15	55.50			101	39.12	0.08	104.35	
	110	59.34	0.4	22.63			110	59.3	0.06	105.85	
30	001	17.7	0.3	26.5	19.05						
	101	38.26	0.47	17.71							
	110	59.46	0.7	12.94							

**Table 4.** Effect of MMH/MMPB on LOI of epoxy resin

Order	1	2	3	4	5	6	7	8	9
Fire retardant		MPB	MH/MPB (0.05:1)*	MH/MPB (0.15:1)*	MH/MPB (0.25:1)*	MH/MPB (0.35:1)*	MH/MPB (0.5:1)*	MH/MPB (0.5:1)*	MH/MPB (0.75:1)*
LOI/%	18	25	27	27	28	26	25	24 (self-extinguish)	24

Note: (\*) is mMh/mMPB.

### 3.7 Effect of mMh/mMPB on LOI of MH/MPB flame-retarded epoxy resin

**Table 4** is the limiting oxygen index of MH/MPB with different mMh/mMPB ratio when adding 20% (mass fraction) to epoxy resin. It can be seen from **Table 4** that MH and MPB have good flame-retarded synergistic effect. When mMh/mMPB is 0.05, the LOI of EP increases from 25% to 27%, and when mMh/mMPB is 0.25, the LOI of EP reaches

the highest point of 28%. With the increase of mMh/mMPB, the amount of MgO produced by hydrolysis is more, which leads to the increase of flame-retarded effect of flame-retarded composites in the combustion process of the flame-retarded composite increased. However, when the mMh/mMPB value exceeds 0.25, the LOI of EP decreased significantly, even lower than that of MPB/EP. The reason may be that there is too much MH, which leads to the rela-

tive reduction of MPB and the impact on its flame retardancy. Therefore, 0.25 mMH/mMPB is the best ratio.

### 3.8 MH/MPB thermogravimetric analysis

According to the TG analysis of MH/MPB (Figure 7), MH/MPB is mainly decomposed at 200–300 °C; after 300 °C, MH/MPB is decomposed very little; at 700 °C, there is still a high carbon residue rate, up to 39%, which shows that MH/MPB has better flame retardancy. The DTG diagram (Figure 8) shows that, MH/MPB has three main thermogravimetric rate peaks 106.2 °C, 261.3 °C and 303.7 °C. Small molecular water contained in MH/MPB shall be at 106.2 °C, 261.3 °C and 303.7 °C are the thermal weight loss rate peaks of MH/MPB. The main peaks of DTA (Figure 9) are 266.9 °C and 317 °C, which is basically consistent with the DTG peak.

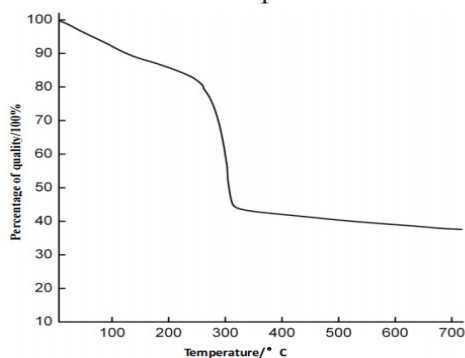


Figure 7. TG pattern of MH/MPB.

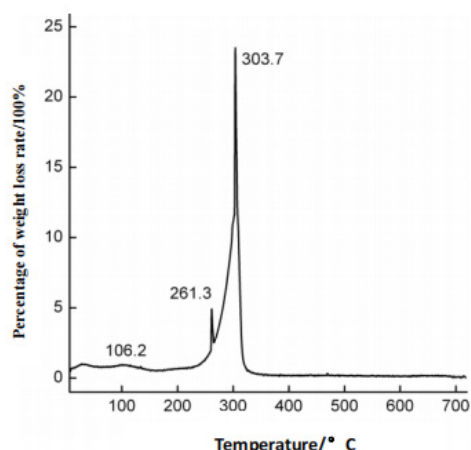


Figure 8. DTG pattern of MH/MPB.

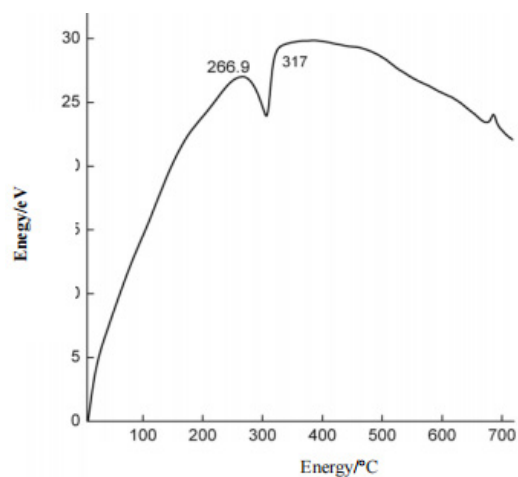


Figure 9. DTA pattern of MH/MPB.

Table 5. Effect of addition amount of MH/MPB (0.25:1)\* on LOI

Order	1	2	3	4	5
Addition amount /%	0	10	20	30	40
LOI /%	18	25	28	29 (self-extinguish)	30

Note: (\*) is mMH/mMPB = 0.25:1.

### 3.9 Preliminary study on the mechanism of MH/MPB flame-retarded epoxy resin

It can be seen from Table 5 that the LOI of MH/MPB/EP is significantly higher than that of EP without MH/MPB (0.25:1)\* (LOI is 18%), and the LOI of EP gradually increases with the increase of MH/MPB addition. When the addition amount reaches 40%, the LOI of epoxy resin reaches 31%. When the addition of MPB was 20%, the LOI of epoxy resin increased significantly, and then tended to be flat. It can be seen that the best addition amount of MH/MPB is 20%, LOI reached 28%. XRD analysis of

carbon residue (Figure 10) shows that the addition of MH makes the peak of carbon residue tend to be flat, and the carbon residue tends to amorphous carbon. So MH changed the morphology of carbon residue.

The carbon slag produced by EP, EP/MPB and EP/MH/MPB in the oxygen index test experiment shall be tested by infrared to understand the carbon layer structure, as shown in Figure 11. By analyzing Figure 11, the infrared spectrum of carbon residue of EP/MH/MPB is obviously different from the other two, and the position of absorption peak changes.

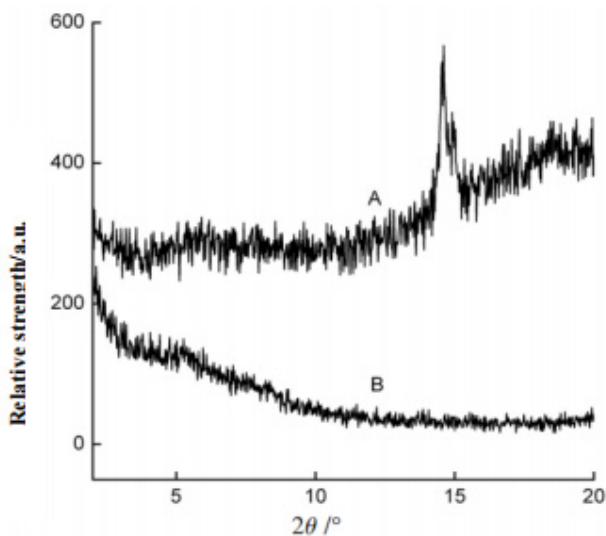


Figure 10. XRD pattern of carbon slag.

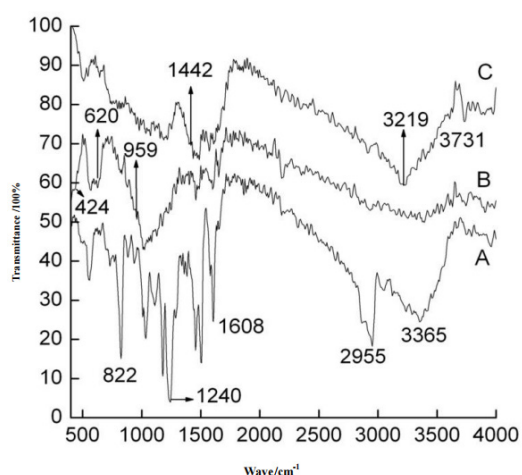


Figure 11. Infrared spectra of EP, EP/MHPB and EP/MH/MPB carbon residues (A: EP; B: EP/MHPB; C: EP/MPB).

In **Figure 11B**, the peak at  $424\text{ cm}^{-1}$  is the stretching vibration absorption peak of Mg-O bond,  $1,317\text{ cm}^{-1}$  is the stretching vibration absorption peak of B-O,  $959\text{ cm}^{-1}$  is the stretching vibration absorption peak of P-O-P,  $1,652\text{ cm}^{-1}$  is the stretching vibration peak of C=C double bond, and  $620\text{ cm}^{-1}$  is the characteristic peak of aromatic ring<sup>[17,23]</sup>. This shows that the combustion carbon residue contains Mg-O bond, B-O bond, P-O-P bond and C=C double bond. In **Figure 11C**, the bi-peaks at  $2,955\text{ cm}^{-1}$  as C=O characteristic peaks disappeared in **Figure 6B**. It is seen that the addition of MH affects the structure and composition of EP combustion carbon slag and the EP combustion thermal decomposition process. During thermal degradation or combustion processes, MH/MPB produces phosphate-poly-

phosphate-polydephosphate, and forms a nonvolatile phosphate layer (P-O-P bond) protective layer. Polydephosphate has dehydration, so it can form the carbonized layer<sup>[24]</sup>; MH/MPB produces boric anhydride or boric acid during combustion. Boric acid can form a glass-like melt (B-O bond) during thermal cracking, which is covered on the material; the combustion carbon residue contains Mg-O bond, B-O bond, P-O-P bond and C=C double bond. In **Figure 11C**, the double peak at  $2,955\text{ cm}^{-1}$  is C=O, and the characteristic peak disappeared in **Figure 6B**. It can be seen that the addition of MH affects the structure and composition of EP combustion carbon slag and the thermal decomposition process of EP combustion. During thermal degradation or combustion or the burning process, MH/MPB produces phosphoric acid–metaphosphoric acid–polymetaphosphoric acid to form a non-volatile phosphoric acid layer (P-O-P bond) protective layer. Polymetaphosphoric acid has dehydration and it can form a carbonization layer<sup>[24]</sup>; during the combustion of MH/MPB, boric anhydride or boric acid is produced. Boric acid can form a glass like molten metal during thermal cracking. The melt (B-O bond) is covered on the material; the high temperature decomposition of MH in MH/MPB produces MgO, which can interact with the pyrolysis products of EP and MPB. It can be transformed into a more stable carbon layer containing Mg, P, B, C and other elements, promote the direct oxidation of the material into carbon dioxide and reduce the combustible gas carbon monoxide. The generation of stable carbon layer can isolate the air and prevent the outward diffusion of combustible gas, so as to achieve the purpose of flame-retarded. In addition, MH/MPB contains nitrogen, which can release refractory gas  $\text{NH}_3$ , when heated, diluting the concentration of oxygen in the air. High temperature MH contained in MH/MPB decomposition endothermic has cooling effect and flame-retarded effect. It can be seen that the flame-retarded EP of MH/MPB has flame-retarded mechanisms such as condensed phase, gas phase and synergy. It can't be explained by one mechanism. It contains nitrogen, which can release refractory gas  $\text{NH}_3$ , when heated, diluting the concentration of oxygen in the air.

## 4. Conclusion

(1) MH/MPB nanocomposite flame-retarded was prepared by in-situ formation method. Through single factor experimental analysis, it is concluded that the grain size of MH/MPB synthesized is small when the reaction temperature is lower than 75 °C and the reaction time is 30 min. It can be seen that MH reaches nano level through Scherrer formula. (2) When mMH/mMPB is 0.25, MH and MPB have the best synergistic effect and the best flame-retarded performance; when the addition amount of epoxy resin (EP) is 20%, the limiting oxygen index (LOI) of epoxy resin reaches 28%. (3) The thermogravimetric analysis of MH/MPB shows that MH/MPB has a high decomposition temperature, and the remaining carbon rate is still 39% at 700 °C. (4) XRD and IR analysis of carbon slag show that the carbon slag contains Mg-O bond, B-O bond, P-O-P bond, C=C double bond and so on. The addition of MH not only plays an endothermic and cooling role, but also makes MH/MPB flame-retarded EP produce stable carbon layer with element structure of Mg, P, B, C and other elements in the combustion process, so as to achieve flame-retarded and heat insulation effect.

## Conflict of interest

The authors declare that they have no conflict of interest.

## References

1. Chen X, Jiao C. Synergistic effects of hydroxy silicone oil on intumescent flame-retarded polypropylene system. *Fire Safety Journal* 2009; 16(44): 1010–1014.
2. Bao Z, Dong Y. Progress in studying expansive flame retardants (in Chinese). *Chemical World* 2006; 47(5): 311–315.
3. Cai Y, Fan H, Chen H, *et al.* Progress in epoxy nano flame-retarded materials (in Chinese). *Thermosetting Resin* 2007; 22(6): 50–53.
4. Marosi G, Marton A, Szep A, *et al.* Fire retardancy effect of migration in polypropylene nanocomposites induced by modified interlayer. *Polymer Degradation and Stability* 2003; 82(2): 379–385.
5. Hu Y, Song L. Flame-retarded polymer nanocomposites (in Chinese). Beijing: Chemical Industry Publishing House; 2008. p. 128–130.
6. Wang Z, Han E, Ke W. Study on improving the water resistance of APP/PER/MEL fire-proof coating (in Chinese). *Journal of Chinese Society for Corrosion and Protection* 2006; 26 (2): 103–107.
7. Wang J, Wang X, Wang W, *et al.* Study on PEPA/nanometer Al(OH)<sub>3</sub> instrument flame-retarded polypropylene. *Plastics Additives* 2006; 56(2): 35–38.
8. Feng C, Zeng Z, Ye J, *et al.* Effect of Nano-SiO<sub>2</sub> on properties of flame retarded PP by MPP/PEPA. *Plastics Science and Technology* 2009; 37(4): 67–70.
9. Mao W, Li Q. Study on the coefficient effect of nano zinc oxide on expanded flame-retarded nylon 66(in Chinese). *Insulating Materials* 2007; 40(3): 32–34.
10. Zhou J, Fang C, Sheng , *et al.* Synergistic action of Nanometer ZnO prepared by sol-gel method on halogen free flame-retarded polypropylene. *Rare Metal Materials and Engineering* 2008; 37(s2): 617–619.
11. Xian C, Meng H, Sun D, *et al.* Application of nanomaterials in fire-proof coatings of water-thin expansion steel structures (in Chinese). *Journal of Material Engineering* 2006; 23(8): 40–44.
12. Liu Z, Ou Y, Wu J. Combustion behaviors of PA6/OMMT nanocomposites flame-retarded by MPP/PER/APP system. *Journal of Functional Polymers* 2004; 17(4): 625–62.
13. Chen M, Wu Z, Hu Y. Research progress of magnesium hydroxide synergistic flame retardants (in Chinese). *Applied Chemical Industry* 2008; 37(8): 939–942.
14. Zhou B, Yang Y. Research status and development trend of magnesium hydroxide flame retardants (in Chinese). *Journal of QiLu Normal University* 2006; 116(4): 100–102.
15. Qu Z, Liu S, Jiang Z, *et al.* Study of the PA6/SAMH/PE ternary compound halogen-free flame-retarded system (in Chinese). *China Plastics Industry* 2009; 37(2): 50–53.
16. Zhao A, Dong Y, Bao Z. Synthesis of phosphate melamine borate flame-retardants (in Chinese). *Shandong Chemical Industry* 2009; 38(12): 1–6.
17. Robert M, Francis X, David J. Spectrometric identi-

- fication of organic compounds. Shanghai: East China University of Science and Technology Press; 2007. p. 101–110.
18. Fan W, Sun S, Song X, *et al.* Controlled synthesis of single-crystalline Mg(OH)<sub>2</sub> nanotubes and nanorods via a solvothermal process. *Journal of Solid State Chemistry* 2004; 177(7): 2329–2338.
  19. Song C, Hu Z, Fu X. Preparation and characterization of Mg(OH)<sub>2</sub> nanosheets. *Journal of Qingdao University of Science and Technology (Natural Science Edition)* 2009; 30(3): 200–202.
  20. Zhang F, Zhang X, Tang Y. Synthesis and synthesis of highly pure ultra-thin sheet nano-magnesium hydroxide (in Chinese). *Fire Protection Technique and Products Information* 2009; (1): 7–9.
  21. Han D, Shi L. Preparation of hydrophobic nano-Mg(OH)<sub>2</sub> by one-step method of alcohol water system. *Chemical Minerals & Processing* 2008; (6): 13–17.
  22. Yin W, Nan L, Han Y, *et al.* Synthesis and crystallization mechanism analysis of nanometer magnesium hydroxide (in Chinese). *Metal Mine* 2005; 345(3): 38–41.
  23. Zhou W, Zhou J, Yang H, *et al.* Flame retardant synergistic effect of nano Mg(OH)<sub>2</sub> and silicone on polypropylene (in Chinese). *Rare Metal Materials & Engineering* 2008; 37(S2): 312–315.
  24. Laoutid F, Bonnaud L, Alexandre M, *et al.* New prospects in flame retardant polymer materials: From fundamentals to nanocomposites. *Materials Science and Engineering: R Reports* 2009; 63(3): 100–125.